NeuroImage 48 (2009) 29–36

Contents lists available at ScienceDirect

NeuroImage

journal homepage: www.elsevier.com/locate/ynimg

Aging of subcortical nuclei: Microstructural, mineralization and atrophy modifications measured in vivo using MRI

Andrea Cherubini [a,*], Patrice Péran [a,b], Carlo Caltagirone [a,c], Umberto Sabatini [a], Gianfranco Spalletta [a]

[a] IRCCS Santa Lucia Foundation, Via Ardeatina, 306, 00179, Rome, Italy
[b] INSERM U825, Toulouse, France
[c] Department of Neuroscience, University of Tor Vergata, Rome, Italy

ARTICLE INFO

Article history:
Received 11 February 2009
Revised 23 April 2009
Accepted 14 June 2009
Available online 21 June 2009

ABSTRACT

In the present study, we characterized the physiological aging of deep grey matter nuclei by simultaneously measuring quantitative magnetic resonance parameters sensitive to complementary tissue characteristics (volume atrophy, iron deposition, microstructural damage) in seven different structures in 100 healthy subjects. Large age-related variations were observed in the thalamus, putamen and caudate. No significant correlations with age were observed in the hippocampus, amygdala, pallidum, or accumbens. Multiple regression analyses of advanced imaging data revealed that the best predictors of physiological aging were the mean relaxation time (T2*) of the putamen and the volume and mean diffusivity of the thalamus. These three parameters accounted for over 70% of the age variance in a linear model comprising 100 healthy subjects, aged from 20 to 70 years. Importantly, the statistical analyses highlighted characteristic patterns of variation for the measurements in the various structures evaluated in this study. These findings contribute in establishing a baseline for comparison with pathological changes in the basal ganglia and thalamus.

Introduction

Deep grey matter (GM) nuclei are involved in processing all physiological behaviours and are affected by the most prevalent neurodegenerative diseases, including Alzheimer's disease, and Parkinson's disease. Because brain aging is a major risk factor for these diseases (Harman, 1991; Farooqui and Farooqui, 2009), it is crucial to characterize the effects of physiological aging on deep GM structures in order to predict when an individual is in the early stages of cognitive decline, and to identify effective ways to slow the normal aging processes.

Modern imaging techniques, such as magnetic resonance (MR), enable researchers to investigate in vivo the progressive structural alterations to brain tissue that accompany physiological aging. Moreover, a variety of MR methods can be applied in order to enhance imaging sensitivity to various structural changes across spatial scales. For example, high-resolution T1-weighted MR images provide sufficient anatomical detail to document the age-related volume shrinkage of cortical and subcortical GM (Pfefferbaum et al., 1994; Good et al., 2001; Fox and Schott, 2004). Using this technique, the pattern and rate of progression of age-related cerebral atrophy can be studied from a macroscopic perspective (on a millimeter scale).

Other techniques, such as Diffusion Tensor Imaging (DTI), can provide a means to noninvasively study tissue microarchitecture and early pathological alterations at the cellular and molecular levels (Basser, 1995; Le Bihan, 1995). In particular, two quantitative parameters derived from DTI have been shown to be greatly influenced by physiological aging. These are mean diffusivity (MD), which increases with the disruption of microscopic barriers and extracellular fluid accumulation, and fractional anisotropy (FA), which provides information about the microstructural integrity of highly oriented microstructures (e.g. myelin) (Abe et al., 2002). MR-based relaxometry techniques can detect the progressive mineralization of deep GM with age, which has been linked with increased risk factors for the most common neurodegenerative diseases (Hallgren and Sourander, 1958; Bartzokis et al., 2007). Indeed, it has been shown that age-related iron deposits can be documented in vivo using MR relaxometry, particularly in deep GM structures such as the striatum and pallidum (Haacke et al., 2005; Péran et al., 2007; Péran et al., in press).

Application of these techniques in age-related studies has produced a considerable amount of information. Nevertheless, the results of previous studies examining subcortical GM structures have often been inconsistent (Liu et al., 2003; Good et al., 2001; Lemaître et al., 2005; Szentkuti et al., 2004; Walhovd et al., 2005). The majority of MR studies of physiological aging in deep GM nuclei to date have concentrated on a single MR technique and/or on a particular anatomical structure in a limited cohort of subjects. However, this approach might be insufficient to fully describe the chain of different structural alterations that modifies the brain tissues simultaneously in different structures with various degrees of intensity. In fact, by selecting a priori a single methodology and/or MR parameter, it is

* Corresponding author. Fax: +39 0651501323.
E-mail address: a.cherubini@hsantalucia.it (A. Cherubini).

1053-8119/$ – see front matter © 2009 Elsevier Inc. All rights reserved.
doi:10.1016/j.neuroimage.2009.06.035

difficult to disentangle the relative proportion of age-related structural alterations in different anatomical locations. In contrast, simultaneously measuring a variety of parameters in a large cohort of subjects across a wide age range would make it possible to gather information that can be used to develop a quantitative profile of physiological aging changes, perhaps interpreting deviations from this profile as a risk factor for neurodegenerative disorders.

The present study was designed to overcome the limitations of previous studies of aging in subcortical GM by measuring simultaneously the volume, DTI scalars, and T2* relaxation rates in seven deep GM structures (thalamus, putamen, hippocampus, caudate, amygdala, pallidum and accumbens) in a large cohort of subjects. We used multiple linear regression analysis to evaluate the relevance, the relative contribution, and the rate of change of these parameters with age. In this context, the present work represents an attempt to characterize, with advanced image analysis procedures and quantitative MR parameters sensitive to complementary brain tissue properties, the physiological aging process in deep GM structures. The primary aim of the present study is to identify the best MR predictor of aging in subcortical GM nuclei.

Methods

Subjects

One hundred healthy subjects (55 women, 45 men; age range 20–70 years; mean age ± standard deviation 41 ± 15 years) provided informed written consent and participated in this study, which was approved by the Santa Lucia Foundation ethics committee. Subjects were recruited from local university colleges, community recreational centers, hospital personnel, and patient's relatives. The selection protocol of eligible participants comprehended a semi-structured interview for the collection of sociodemographic and anamnesis data regarding current and past clinical history.

All subjects were assessed by one senior clinical psychiatrist using the Structured Clinical Interviews for DSM-IV Axis I (SCID-NP) and Axis II (SCID-II). Exclusion criteria in the selection of participating individuals included i) no dementia diagnosis or cognitive deterioration according with NINCDS-ADRDA criteria (McKhann et al., 1984), confirmed by the administration of the Mental Deterioration Battery (MDB) (Carlesimo et al., 1996), or Mini-Mental State Examination (MMSE) (Folstein et al., 1975) score higher or equal than 26, consistently with normative data in the Italian population (Measso et al., 1993); ii) no mental retardation according with DSM-IV criteria; iii) subjective complain of memory difficulties or of any other cognitive deficits, interfering or not with the daily living activities; iv) major medical illnesses, e.g., diabetes (not stabilized), obstructive pulmonary disease, or asthma; hematologic and oncologic disorders; pernicious anaemia; clinically significant and unstable active gastrointestinal, renal, hepatic, endocrine, or cardiovascular system disease; newly treated hypo-thyroidism; v) current or reported psychiatric or neurologic disorders (e.g., schizophrenia, major depression, stroke, Parkinson disease, seizure disorder, head injury with loss of consciousness) and any other significant mental or neurological disorder; vi) known or suspected history of alcoholism or drug dependence and abuse during lifetime.

Two expert radiologists examined all MR images to exclude potential brain abnormalities and subjects with microvascular lesions as apparent in conventional FLAIR and T2-weighted images. These volunteers were examined using a 3 T Allegra MR Imager (Siemens Medical Solutions, Erlangen, Germany) with a standard quadrature head coil.

Acquisition

Participants underwent the same MR imaging protocol including whole-brain T2*-weighted, T1-weighted, DTI, conventional T2-weighted and fluid-attenuated inversion recovery (FLAIR) scanning. All planar sequence acquisitions were acquired along the anterior/posterior commissure line. Particular care was taken to center the subject in the head coil and to restrain the subject's movements with cushions and adhesive medical tape. Six consecutive T2*-weighted gradient-echo whole-brain volumes were acquired using a segmented echo-planar imaging sequence at different TEs: 6, 12, 20, 30, 45, and 60 ms (TR = 5000; bandwidth = 1116 Hz/vx; matrix size 128 × 128; 80 axial slices; flip angle 90°; voxel size of 1.8 × 1.8 × 1.8 mm^3). Diffusion-weighted volumes were acquired using spin-echo echo-planar imaging (TE/TR = 89/8500 ms, bandwidth = 2126 Hz/vx; matrix size 128 × 128; 80 axial slices, voxel size 1.8 × 1.8 × 1.8 mm^3) with 30 isotropically distributed orientations for the diffusion-sensitising gradients at a *b*-value of 1000 $s \cdot mm^2$ and 6 $b = 0$ images. Scanning was repeated three times to increase the signal-to-noise ratio. Since DTI and T2* volumes both consisted of 128 × 128 × 80 identical isotropic voxels, the slice positioning and orientation of the diffusion-weighted volumes were set to be identical with the T2* volumes in order to improve subsequent coregistration. Finally, whole-brain T1-weighted images were obtained in the sagittal plane using a modified driven equilibrium Fourier transform (MDEFT) (Deichmann et al., 2004) sequence (TE/TR = 2.4/7.92 ms, flip angle 15°, voxel size 1 × 1 × 1 mm^3).

Post-processing

Image processing was performed using FSL 4.1 (www.fmrib.ox.ac.uk/fsl/) and an in-house developed software in Matlab (vers. 6.5, the MathWorks) with procedures similar to those described in previous works (Cherubini et al., 2009; Péran et al., in press). Anatomical regions of interest (ROI) on T1-weighted images were obtained automatically with the segmentation tool FIRST 1.1 integrated within the FSL software. FIRST uses mesh models trained with a large amount of rich hand-segmented training data to segment subcortical structures. This method of segmentation is particularly useful for structures with a low contrast-to-noise ratio. In each subject, the following seven deep grey matter structures were segmented: thalamus, putamen, hippocampus, caudate, amygdala, pallidum, and accumbens.

Image distortions induced by eddy currents and head motion in the DTI data were corrected by applying a 3D full affine (mutual information cost function) alignment of each image to the mean no diffusion weighting (*b*0) image. After distortion corrections, DTI data were averaged and concatenated into thirty-one (1 *b*0 + 30 *b*1000) volumes. A diffusion tensor model was fit at each voxel, generating fractional anisotropy (FA) and mean diffusivity (MD) maps. The FA maps created were then registered to brain-extracted whole-brain volumes from T1-weighted images using a full affine (correlation ratio cost function) alignment with nearest-neighbour resampling. The calculated transformation matrix was then applied to the MD maps with identical resampling options.

The six T2*-weighted volumes were averaged in order to generate a mean T2*-weighted volume. A full affine 3D alignment was calculated between each of the six T2*-weighted volumes and the mean T2*-weighted volume. For each subject we performed a voxel-by-voxel nonlinear least-squares fitting of the data acquired at the six TEs to obtain a mono-exponential signal decay curve ($S = S_0 e^{-t/T2^*}$). In order to facilitate analysis of relaxation results, we considered the inverse of relaxation times, i.e. relaxation rates $R2^* = 1/T2^*$ as described in previously published works (Cherubini et al., 2009; Péran et al., 2007; Péran et al., in press). The mean T2*-weighted volume was registered to the T1-weighted volume using a full affine (correlation ratio cost function) alignment. The calculated transformation matrix was then applied to the R2* maps with nearest-neighbour resampling options. As a result of this processing, MD, FA, and R2* maps were corrected for head movements, and shared an

identical reference space with the anatomical T1-weighted volumes (Fig. 1).

For each subject, the results of ROI segmentation, the coregistered FA map, and the coregistered R2* map were all superimposed to the original T1-weighted volume (Fig. 1), and the resulting images were visually assessed by two trained radiologists to exclude misregistration or erroneous ROI identification. For each subject and each hemisphere, the volumes of the segmented subcortical areas were calculated. In order to reduce the effects of inter-individual variability in head size, individual volume values were multiplied by a normalization factor obtained with the SIENAX tool (http://www.fmrib.ox.ac.uk/fsl/siena/index.html) from the corresponding T1-weighted image. This normalization factor is derived from the normalizing transform, i.e. the brain image is affine registered to a template and a multiplying factor is calculated from the transformation matrix itself (using the skull image to determine the registration scaling). Since the investigation of lateralization effects were not within the main aims of the present work, adjusted volumes from bilateral ROIs for each subject were averaged prior to statistical analyses. The segmented structures defined the binary masks where mean values of MD, FA and R2* were calculated for each individual.

Statistical analysis

Data from all 100 subjects were included in the statistical analyses. For each of the seven deep GM structures, we considered the following quantitative predictors: volume, mean R2*, mean MD and mean FA. First, we calculated the Pearson correlation coefficient between each of these parameters and age in the single ROIs. Second, we calculated the correlation coefficients between the four predictors within each of the seven ROI. Subsequently, we performed a multiple regression analysis according to the following linear model: age = beta × [predictors] + constants. We adopted $p<0.05$ with Bonferroni corrections as statistical thresholds throughout the study.

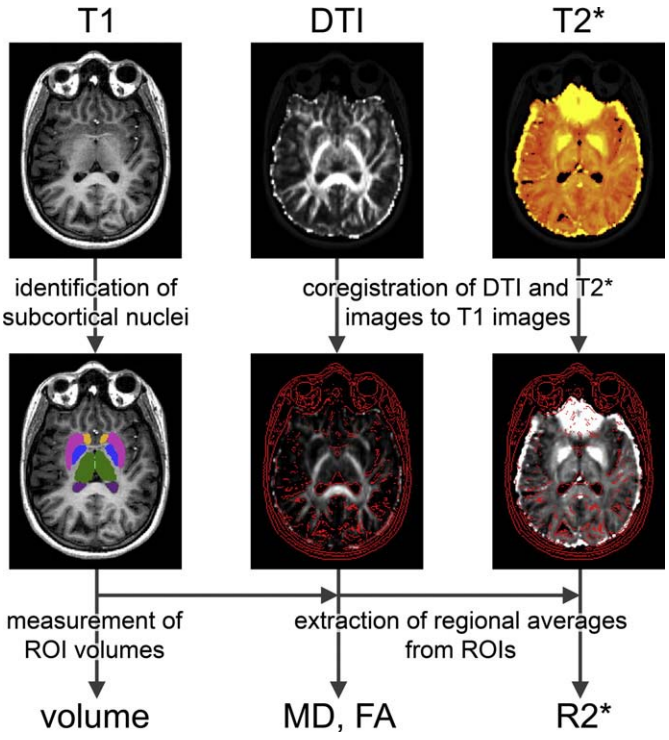

Fig. 1. A schematic representation of the image analysis process. Subcortical structures are identified on T1-weighted volumes, while DTI volumes and R2* maps are coregistered to T1-weighted volumes. Volume of ROIs are corrected for intracranial volume, while the same ROIs are used to extract regional averages of MD, FA and R2* values.

Results

Correlations between age and brain measures

As shown in Fig. 2, correlational analysis revealed a positive correlation of age with both MD and R2*, as well as a negative correlation of age with volume, in both striatal structures (caudate and putamen). Similarly, in the thalamus, we observed significant volume shrinkage and MD increase with age. No significant R2* variation was observed in the thalamus. There were no correlations between age and each of the four stated parameters in the hippocampus, amygdala, globus pallidus, and accumbens (Bonferroni correction, $p<0.05/28$).

Examination of potential cross correlations (Table 1) between the four MR predictors within each ROI revealed significant negative correlations between the two parameters derived from the diffusion tensor (MD and FA) in most of the target structures, namely the thalamus, hippocampus, amygdala, pallidum and accumbens. We also observed a positive correlation between R2* and MD in the putamen ($R=0.34$; $p<0.001$) and a negative correlation between volume and MD in the caudate ($R=-0.37$; $p<0.001$).

Multiple linear regression analyses

In order to evaluate the relative contribution of each of the four parameters to aging in a particular structure, we performed a regression analysis for each ROI using a multiple linear model including all four predictors. In other words, for each structure we modelled age as a linear combination of the four predictors measured within each ROI. The regression coefficients of this statistical analysis are shown in Table 2. The age variance explained by the linear model was greater than 50% in the thalamus, putamen and caudate. The remaining four subcortical structures did not make a significant contribution. The FA does not appear to contribute significantly to the model in any of the considered structures.

In each of the three subcortical structures where we observed a correlation with age, the MD contributed appreciably to the linear model. Volume shrinkage appeared to be important in the thalamus but not in the striatum (putamen + caudate). On the other hand, this latter pattern was reversed in the striatum where the best predictor of age, together with MD, resulted in the relaxation rate rather than the volume.

The six significant structure/parameter pairs resulting from the regression analysis described above (Table 2) were fed into a novel multiple regression analysis. In other words, we considered a new analysis where age could be calculated from a combination of the following predictors: $\text{thalamus}_{\text{Volume}}$, $\text{thalamus}_{\text{MD}}$, $\text{putamen}_{\text{R2*}}$, $\text{putamen}_{\text{MD}}$, $\text{caudate}_{\text{R2*}}$, and $\text{caudate}_{\text{MD}}$. The results of this analysis showed that the best predictors of aging were the volume (beta = −0.300) and MD (beta = 0.315) of the thalamus, as well as R2* in the putamen (beta = 0.541) (Fig. 3). The remaining three factors did not act as significant predictors of aging. As shown in Fig. 4, considering only the best three predictors was sufficient to explain the age variance to the level of $R^2=0.73$.

Discussion

In this study we characterized physiological aging in deep GM nuclei by simultaneously measuring four MR parameters sensitive to complementary tissue characteristics (volume atrophy, iron deposition, microstructural damage) in seven structures (thalamus, putamen, hippocampus, caudate, amygdala, pallidum and accumbens) in a large cohort of healthy subjects. The combination of advanced imaging techniques and multiple regression analyses revealed that, overall, the best predictors of physiological aging were the mean relaxation time (T2*) of the putamen and the volume and mean diffusivity of the

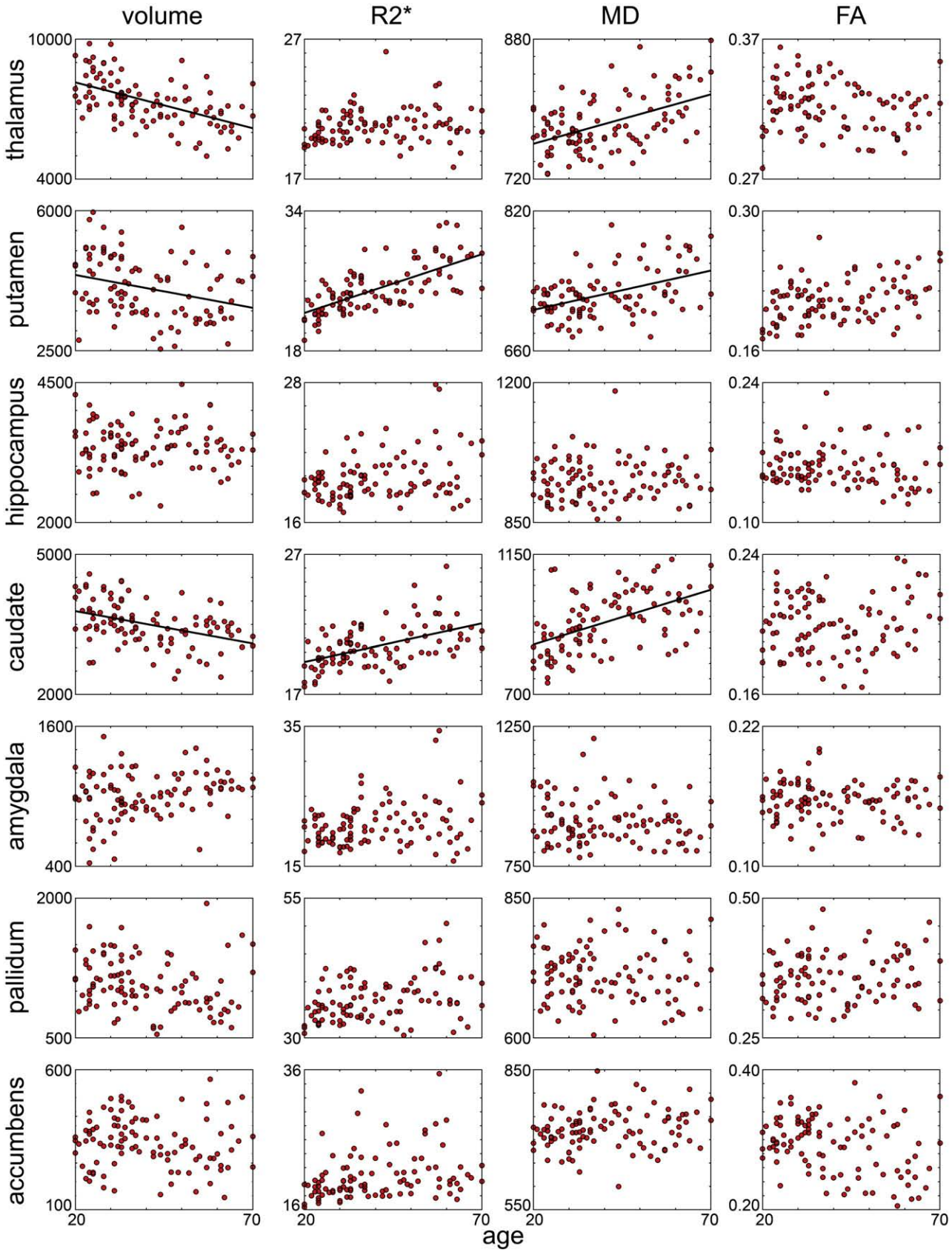

Fig. 2. Scatter plots of each bilateral normalized volume [mm^3], mean R2* [s^{-1}], mean MD [$10^{-6} mm^2 s^{-1}$], and mean FA vs. age for the seven deep GM structures considered in this work. A regression line is plotted for those correlation analyses where we observed a significant correlation with age (Bonferroni correction; $p<0.05/28$).

Table 1
Inter-correlation coefficients between the four MR predictors (volume, R2*, MD, FA) within each of the subcortical structure.

	Volume vs. R2*		Volume vs. MD		Volume vs. FA		R2* vs. MD		R2* vs. FA		MD vs. FA	
	R	*p*	*R*	*p*	*R*	*p*	*R*	*p*	*R*	*p*	*R*	*p*
Thalamus	−0.150	0.137	−0,007	0.948	0.105	0.300	−0.111	0.273	0.052	0.610	**−0.403**	**0.000**
Putamen	−0.172	0.088	−0.225	0.024	0.257	0.010	**0.341**	**0.001**	0.304	0.002	−0.021	0.834
Hippocampus	0.245	0.014	0.183	0.068	0.074	0.467	0.167	0.097	0.167	0.098	**−0.401**	**0.000**
Caudate	−0.076	0.450	**−0.370**	**0.000**	−0.067	0.511	0.165	0.100	0.208	0.038	−0.270	0.007
Amygdala	0.169	0.093	−0.076	0.454	−0.030	0.764	0.263	0.008	−0.278	0.005	**−0.580**	**0.000**
Pallidum	−0.190	0.059	0.305	0.002	−0.133	0.188	−0.107	0.289	0.215	0.032	**−0.711**	**0.000**
Accumbens	−0.110	0.278	−0.100	0.320	0.089	0.380	−0.052	0.605	0.271	0.006	**−0.496**	**0.000**

Structures where the correlation is significant are highlighted in bold (Bonferroni correction; $p<0.05/42$).

thalamus. These three parameters alone accounted for over 70% of the age variance in a linear model comprised of 100 healthy controls aged 20 to 70 years. Notably, the statistical analyses highlighted interesting patterns of variation for the measurements in the different structures considered in this work. In the following sections, we will discuss the results grouping the structures according to these patterns.

Thalamus

In the thalamus, both volume and MD correlated with age (Fig. 2). However, volume and MD did not correlate with each other within the structure itself (Table 1). In the multiple regression, the two parameters together explained 57% of the age variance in the thalamus, with regression coefficients beta = −0.53 and beta = 0.56, respectively (Table 2). Considering these results together, it appears that R2* and FA are not significantly linked to age, whereas both volume and MD are critically important in the aging process of the thalamus, consistently with previous literature (Good et al., 2001; Walhovd et al., 2005; Abe et al., 2008; Pfefferbaum et al., in press).

The absence of a significant R2* correlation with age is not unexpected given that the metal deposition rate for the thalamus is certainly smaller than that of other nuclei, such as the caudate or putamen (Hallgren and Sourander, 1958). By contrast, the unanticipated result is that volume and MD appear to be independent of each other within the structure. These results seem to suggest that the measurements of MD and volume for this structure correspond to different, although linked, biological phenomena.

The biological underpinning of both the MD increase and volume shrinkage is thought to be the continuous deterioration of neuronal structures, which in the case of physiological aging might be evidenced by an increase of extracellular space due to shrinkage of neuronal soma and/or neuronal death (Basser, 1995). The primary difference between diffusivity and volume is that the first parameter is sensitive to structural variations at the cellular and molecular level (Le Bihan, 1995), while the latter is a measure of macroscopic structural characteristics. Thus, we could speculate that although the variations of the two parameters in the thalamus might share a common cause, the effects of the deterioration of neuronal structure produce different effects at different spatial scales. These results highlight the importance of measuring both parameters when investigating the disruption of tissue within the thalamus.

A recent study (Pfefferbaum et al., in press) that measured DTI and iron-related parameters (field dependent relaxation rate, FDRI) in deep GM nuclei yielded a negative correlation between diffusivity and mineralization for the thalamus. By contrast, we did not observe significant correlations between R2* and MD within the thalamus. The difference between the two findings could be due to differing age ranges and dimensions of the subject groups. The former study involved 10 young adult subjects (22–37 years of age) and 7 relatively older adult subjects (65–79 years of age), while our study examined 100 subjects whose ages were evenly distributed between 20 and 70 years.

In another recent study (Abe et al., 2008) that measured age-related diffusivity and volumetric differences in 73 female subjects with a voxel-based approach, the authors reported a decrease in FA accompanying the decrease in volume and the increase in MD in the thalamus. We could observe a similar trend in the scatter plot in Fig. 2, although the correlation between FA and age did not reach significance. Since it has been suggested (Abe et al. 2008; Pfefferbaum et al., in press) that the increase of MD in the thalamus might be due to its lower proportion of large volume components (neurons and myelinated axons), this might be true also for the decrease in FA, which is also strongly correlated with MD (Table 1) in this structure.

Putamen and caudate

The patterns observed in the putamen and caudate differed dramatically from that observed in the thalamus. Age was strongly correlated in both striatal structures with volume, MD and R2* (Fig. 2). These changes were not independent from each other, as there was a positive correlation between R2* and MD in the putamen, and a negative correlation between volume and MD in the caudate (Table 1). The multiple regression analysis demonstrated that the best predictors of aging in these nuclei were R2* and MD rather than structure volume. However, while the largest regression coefficient in the caudate was diffusivity, the situation was reversed in the putamen, with relaxometry providing the best predictor of aging variation (Table 2).

Table 2
Regression coefficients of the multiple linear model: age = beta × [predictors] + constants applied to each structure.

	R^2	Volume		R2*		MD		FA	
		beta	*p*	beta	*p*	beta	*p*	beta	*p*
Thalamus	**0.572**	**−0.529**	**0.000**	0.136	0.050	**0.560**	**0.000**	0.112	0.133
Putamen	**0.617**	−0.233	0.002	**0.466**	**0.000**	**0.256**	**0.000**	0.273	0.002
Hippocampus	0.132	−0.081	0.424	0.367	0.004	−0.047	0.668	−0.188	0.088
Caudate	**0.523**	−0.216	0.007	**0.395**	**0.000**	**0.415**	**0.000**	0.137	0.082
Amygdala	0.139	0.200	0.044	0.251	0.015	−0.199	0.097	−0.073	0.541
Pallidum	0.161	−0.177	0.084	0.281	0.005	0.221	0.122	0.234	0.094
Accumbens	0.228	−0.008	0.933	0.386	0.005	0.013	0.904	−0.394	0.003

Structures where the model is significant are highlighted in bold (Bonferroni correction; $p<0.05/28$).

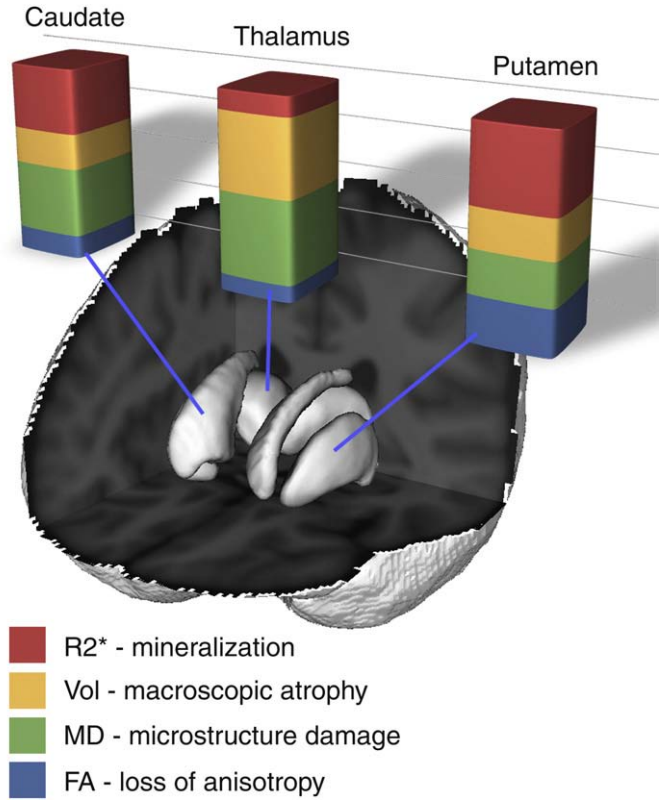

Fig. 3. Relative proportion of structural variations in the three nuclei where most of the age-related effects were observed. Progressive mineralization represents the best age predictor in the striatum (caudate and putamen), while volume atrophy and increasing diffusivity are the best predictors in the thalamus.

Taken together these data suggest that, in the striatum, there is a strong effect of aging, which is clearly evidenced in all our MR measurements. The similar trend of these correlations suggests that these age-related changes might all share a similar physiological genesis, but with different relative intensities upon the two nuclei of the striatum. Although we observed volume shrinkage of both structures, this atrophy seems not to be the main effect of aging. Indeed, R2* in the putamen and MD in the caudate, rather than structure volume, were the best predictors of age-related structural changes in the striatum.

The precise etiology of volume reduction and increased MD in the striatum is unknown, although our observations are in good agreement with previous findings (Good et al., 2001; Walhovd et al., 2005; Abe et al., 2008). In particular, our results are consistent with previous works which demonstrated how relaxation rates, such as R2*, are heavily influenced by local metal depositions (mainly iron), which are particularly intense in the striatum (Haacke et al., 2005; Péran et al., 2007; Péran et al., in press). In fact, it is well documented that mineral content increases in the basal ganglia, although the mechanisms underlying this progressive iron deposition are not well understood. The early work of Hallgren and Sourander (1958) showed that iron increases more slowly in the putamen and caudate than in other structures, levelling off in the sixth decade of life. This might be the reason why the linear model of the R2* increase with age appears particularly robust in the striatum, especially in the putamen.

The cross-correlation between R2* and MD in the putamen suggests that the progressive iron deposition and microstructural damage observed within the putamen may be affiliated phenomena. In fact, it is believed that the destruction of gray matter causes the release of iron, which is then taken up by activated microglia (Harder et al., 2008). Mineral deposits may, in turn, restrict blood flow and cause neural tissue injury that leads to further iron deposition.

In the caudate, where we observed a stronger correlation between age and MD rather than with R2*, the age-related atrophy appeared more relevant when compared to the accumulation of iron. Indeed, the cross-correlation between volume and MD within the caudate could be an indication of this atrophy occurring both at a macroscopic and at a microscopic spatial scale in this nucleus.

Hippocampus, amygdala, pallidum, accumbens

We did not find significant variations of any of our MR parameters in the hippocampus, amygdala, pallidum and accumbens. These findings are not altogether surprising given that, although these structures are surely affected by age-related changes, the higher variability of MR parameters between individuals of similar age makes it difficult to link the parameters to a single variable such as subject age. Indeed this high inter-individual variability may explain why previous studies of aging in these structures have been inconsistent (Good et al. 2001; Liu et al., 2003; Szentkuti et al., 2004; Walhovd et al., 2005). For example, it was recently reported that hippocampal volume is as variable in young healthy adults as it is in old healthy adults (Lupien et al., 2007). In a very large-scale study (Good et al., 2001), amygdalar and hippocampal volumes were found to be preserved relative to that of other GM structures. The limited spatial extension of the amygdala, pallidum, and accumbens can affect the precision of image analyses, exacerbating small errors of identification and coregistration of different MR modalities. Moreover, volume values in previous works were not always corrected for intracranial volume differences, adding additional variability to the results. For example, age-related atrophy of hippocampus and amygdala was observed when volume values were not corrected for global brain volume (Walhovd et al., 2005). This might indicate a relative preservation of these structures relative to global grey matter volume.

Combined multiple regression across different structures

When we considered a multiple regression analysis comprising the factors observed in the various structures, it emerged that the best predictors of aging across structures were the relaxation rate in the

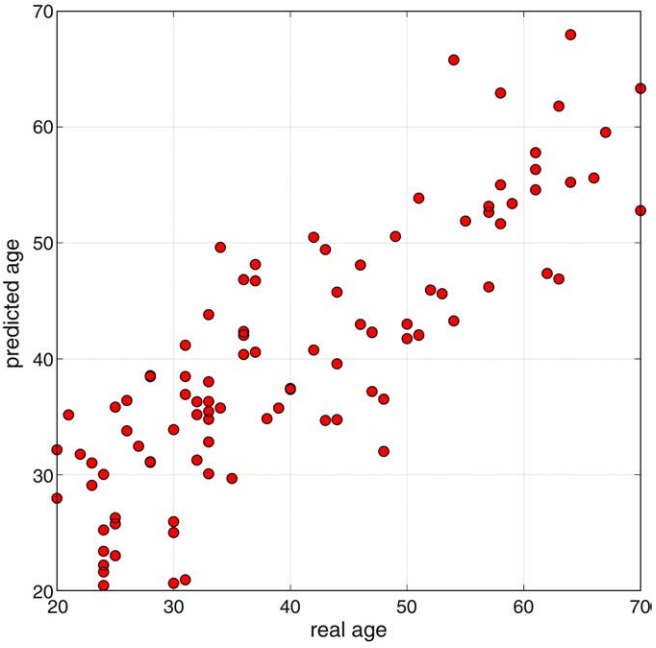

Fig. 4. Plot of real age vs. the age predicted using only thalamus volume, thalamus MD and R2* in the putamen as predictors. These three parameters are capable of explaining over 70% of age variance in a cohort of 100 healthy aged from 20 to 70 years.

putamen and volume and diffusivity in the thalamus. This is a remarkable result given that the combination of these measurements suggested a reproducible trend of linear structural changes across a large cohort of subjects (Fig. 4). A wide range of normal variation in any measure poses huge challenges for the use of that measure in clinical settings. The fact that, in this study, we observed dense, strong, and consistent relationships with age for the three factors mentioned above represents a promising start for delineating a physiological profile of age changes involving multiple parameters.

Our result is even more surprising in light of the fact that we did not extend the analyses to other tissues known to be affected by aging, such as cortical GM or white matter fibre bundles (Good et al., 2001; Walhovd et al., 2005; Abe et al., 2008). The scatter plot in Fig. 4 might well improve if we extend the multiple regression analysis to different anatomical structures and to other quantitative parameters. If this proves to be the case, we may be capable of guessing the "apparent" age of a brain, or of interpreting deviations from this physiological profile as a risk factor for neurodegenerative diseases.

Limitations

The absence of significant age-related variations of FA with age suggests that this parameter might not be the optimum for studying structural changes in subcortical grey matter structures. This could be expected, given that this parameter has been ideated for investigating white matter fibre bundles where tissue disruption can induce loss of local spatial anisotropy. However, the trends that we observed in the thalamus and striatum are in good agreement with previous findings (Abe et al., 2008).

Ideally, investigations of brain aging would be based on observed changes over time in individual subjects. However, it is not practical to perform such longitudinal studies due to a number of logistical complications. Thus, the cross-sectional data presented here describe differences between subjects of different ages, rather than describing changes correlated with aging within individual subjects. This approach has inherent limitations as there is the potential for confounding age and cohort effects, and biases due to differences in physique.

Since we analysed a large cohort of subjects, we attempted to retain the anatomical precision of ROI-based approaches by outlining the brain structures of interest within each individual. At the same time, we tried to maintain the capability of voxel-based approaches to analyse many images by fully automating the post-processing procedures. Nevertheless, it remains a challenge to obtain perfect segmentation of anatomical nuclei and coregistration of different images. In order to minimise these inaccuracies, we individually checked all images for erroneous identification of the structures or misalignment of the MR volumes.

Several studies have reported quadratic or generally nonlinear variations of volumes and relaxation rates with age (Bartzokis et al., 2004; Walhovd et al., 2005). Thus, fitting age variations with linear models might constitute an over-simplification. However, when observing the scatter plots in Fig. 2, we could not detect any consistent break point across measures or structures. Such nonlinear effects could become more pronounced if the subject age range were expanded to include individuals older than 70 or younger than 20.

Conclusions

In this study, we combined advanced imaging techniques and multiple regression analyses in order to identify the best predictors of aging in subcortical GM nuclei. Our results revealed that overall the best predictors of physiological aging were iron deposition in the putamen, and microstructural damage and atrophy in the thalamus. The combination of measurements sensitive to these phenomena suggested a reproducible trend of linear structural changes across 100 healthy subjects aged from 20 to 70 years. The dense, strong and consistent relationships observed with age for the three factors mentioned above may represent a promising start for delineating a physiological profile of age changes involving multiple parameters. If this proves to be the case, we may be able to use these results to estimate the "apparent" age of a brain, or to interpret deviations from this physiological profile as a risk factor for neurodegenerative diseases.

Acknowledgments

We are grateful to Dr. Giacomo Luccichenti for helpful discussion and neuroradiological evaluation of the MRI data sets, and to all our volunteers for their participation. This work was supported in part by grants from the Italian Ministry of Health (RC05-06-07-08-09/A; RF-06; PS-05).

References

Abe, O., Aoki, S., Hayashi, N., Yamada, H., Kunimatsu, A., Mori, H., et al., 2002. Normal aging in the central nervous system: quantitative MR diffusion-tensor analysis. Neurobiol. Aging 23 (3), 433–441.

Abe, O., Yamasue, H., Aoki, S., Suga, M., Yamada, H., Kasai, K., et al., 2008. Aging in the CNS: comparison of gray/white matter volume and diffusion tensor data. Neurobiol. Aging 29 (1), 102–116.

Bartzokis, G., Sultzer, D., Lu, P., Nuechterlein, K., Mintz, J., Cummings, J., 2004. Heterogeneous age-related breakdown of white matter structural integrity: implications for cortical "disconnection" in aging and Alzheimer's disease. Neurobiol. Aging 25 (7), 843–851.

Bartzokis, G., Tishler, T., Lu, P., Villablanca, P., Altshuler, L., Carter, M., et al., 2007. Brain ferritin iron may influence age- and gender-related risks of neurodegeneration. Neurobiol. Aging 28 (3), 414–423.

Basser, P., 1995. Inferring microstructural features and the physiological state of tissues from diffusion-weighted images. NMR Biomed. 8 (7–8), 333–344.

Carlesimo, G.A., Caltagirone, C., Gainotti, G., 1996. The mental deterioration battery: normative data, diagnostic reliability and qualitative analyses of cognitive impairment. The Group for the Standardization of the Mental Deterioration Battery. Eur. Neurol. 36, 378–384.

Cherubini, A., Péran, P., Hagberg, G., Varsi, A., Luccichenti, G., Caltagirone, C., et al., 2009. Characterization of white matter fiber bundles with T2* relaxometry and diffusion tensor imaging. Magn. Reson. Med. 61 (5), 1066–1072.

Deichmann, R., Schwarzbauer, C., Turner, R., 2004. Optimisation of the 3D MDEFT sequence for anatomical brain imaging: technical implications at 1.5 and 3 T. NeuroImage 21 (2), 757–767.

Farooqui, T., Farooqui, A., 2009. Aging: an important factor for the pathogenesis of neurodegenerative disease. Mech. Ageing Dev. 130 (4), 203–215.

Folstein, M.F., Folstein, S.E., McHugh, P.R., 1975. "Mini-mental state". A practical method for grading the cognitive state of patients for the clinician. J. Psychiatr. Res. 12 (3), 189–198.

Fox, N., Schott, J., 2004. Imaging cerebral atrophy: normal ageing to Alzheimer's disease. Lancet 363 (9406), 392–394.

Good, C., Johnsrude, I., Ashburner, J., Henson, R., Friston, K., Frackowiak, R., 2001. A voxel-based morphometric study of ageing in 465 normal adult human brains. NeuroImage 14 (1 Pt 1), 21–36.

Haacke, E., Cheng, N., House, M., Liu, Q., Neelavalli, J., Ogg, R., et al., 2005. Imaging iron stores in the brain using magnetic resonance imaging. Magn. Reson. Imaging 23 (1), 1–25.

Hallgren, B., Sourander, P., 1958. The effect of age on the non-haemin iron in the human brain. J. Neurochem. 3, 41–51.

Harder, S., Hopp, K., Ward, H., Neglio, H., Gitlin, J., Kido, D., 2008. Mineralization of the deep gray matter with age: a retrospective review with susceptibility-weighted MR imaging. Am. J. Neuroradiol. 29 (1), 176–183.

Harman, D., 1991. The aging process: major risk factor for disease and death. Proc. Natl. Acad. Sci. U. S. A. 88 (12), 5360–5363.

Le Bihan, D., 1995. Molecular diffusion, tissue microdynamics and microstructure. NMR Biomed. 8 (7–8), 375–386.

Lemaître, H., Crivello, F., Grassiot, B., Alpérovitch, A., Tzourio, C., Mazoyer, B., 2005. Age- and sex-related effects on the neuroanatomy of healthy elderly. NeuroImage 26 (3), 900–911.

Liu, R., Lemieux, L., Bell, G., Sisodiya, S., Shorvon, S., Sander, J., et al., 2003. A longitudinal study of brain morphometrics using quantitative magnetic resonance imaging and difference image analysis. NeuroImage 20 (1), 22–33.

Lupien, S., Evans, A., Lord, C., Miles, J., Pruessner, M., Pike, B., et al., 2007. Hippocampal volume is as variable in young as in older adults: implications for the notion of hippocampal atrophy in humans. NeuroImage 34 (2), 479–485.

McKhann, G., Drachman, D., Folstein, M., Katzman, R., Price, D., Stadlan, E.M., 1984. Clinical diagnosis of Alzheimer's disease: report of the NINCDS-ADRDA Work Group under the auspices of Department of Health and Human Services Task Force on Alzheimer's Disease. Neurology 34 (7), 939–944.

Measso, G., Caverzeran, F., Zappala`, G., Lebowitz, B.D., Crook, T.H., Pirozzolo, F.J., Amaducci, L., Masari, D., Grigoletto, F., 1993. The mini-mental state examination: normative study of an Italian random sample. Dev. Neuropsychol. 9 (2), 77–85.

Péran, P., Hagberg, G., Luccichenti, G., Cherubini, A., Brainovich, V., Celsis, P., et al., 2007. Voxel-based analysis of R2* maps in the healthy human brain. J. Magn. Reson. Imaging: JMRI 26 (6), 1413–1420.

Péran, P., Cherubini, A., Luccichenti, G., Hagberg, G., Démonet, J., Rascol, O., et al., in press. Volume and iron content in basal ganglia and thalamus. Human Brain Mapping. doi:10.1002/hbm.20698.

Pfefferbaum, A., Mathalon, D., Sullivan, E., Rawles, J., Zipursky, R., Lim, K., 1994. A quantitative magnetic resonance imaging study of changes in brain morphology from infancy to late adulthood. Arch. Neurol. 51 (9), 874–887.

Pfefferbaum, A., Adalsteinsson, E., Rohlfing, T., and Sullivan, E., in press. Diffusion tensor imaging of deep gray matter brain structures: Effects of age and iron concentration. Neurobiology of Aging. doi:10.1016/j.neurobiolaging.2008.04.013.

Szentkuti, A., Guderian, S., Schiltz, K., Kaufmann, J., Münte, T., Heinze, H.J., et al., 2004. Quantitative MR analyses of the hippocampus: unspecific metabolic changes in aging. J. Neurol. 251 (11), 1345–1353.

Walhovd, K., Fjell, A., Reinvang, I., Lundervold, A., Dale, A., Eilertsen, D., et al., 2005. Effects of age on volumes of cortex, white matter and subcortical structures. Neurobiol. Aging 26 (9), 1261–1270 discussion 1275–8.